JOURNAL OF AGRICULTURAL AND FOOD CHEMISTRY

J. Agric. Food Chem. **2007,** *55,* 903–911 **903**

DFT Study of Quercetin Activated Forms Involved in Antiradical, Antioxidant, and Prooxidant Biological Processes

SÉBASTIEN FIORUCCI, JÉRÔME GOLEBIOWSKI, DANIEL CABROL-BASS, AND SERGE ANTONCZAK*

Laboratoire de Chimie des Molécules Bioactives et des Arômes, UMR-CNRS 6001, Faculté des Sciences,Université de Nice-Sophia Antipolis, 06108 Nice Cedex 2, France

Quercetin, one of the most representative flavonoid compounds, is involved in antiradical, antioxidant, and prooxidant biological processes. Despite a constant increase of knowledge on both positive and negative activities of quercetin, it is unclear which activated form (quinone, semiquinone, or deprotonated) actually plays a role in each of these processes. Structural, electronic, and energetic characteristics of quercetin, as well as the influence of a copper ion on all of these parameters, are studied by means of quantum chemical electronic structure calculations. Introduction of thermodynamic cycles together with the role of coreactive compounds, such as reactive oxygen species, gives a glimpse of the most probable reaction schemes. Such a theoretical approach provides another hint to clarify which reaction is likely to occur within the broad range of quercetin biological activities.

KEYWORDS: Quercetin; flavonoid; reactivity indices; electronic structures; solvent effect

INTRODUCTION

Flavonoids are natural compounds present in a large variety of plants, fruits, and vegetables daily eaten by human beings (*1*−*4*). Increasing the knowledge about flavonoids' biodisponibility is a domain of research still in development, as reflected by numerous recent publications (*5*−*7*). Their biochemical and physiological activities are nowadays well recognized and intensively studied (*8*−*10*). Flavonoids behave as antioxidants by a variety of ways including direct trapping of reactive oxygen species (ROS), inhibition of enzymes responsible for superoxide anion production, chelation of transition metal ions involved in processes forming radicals, and prevention of the peroxidation process by reducing alkoxyl and peroxyl radicals (*11*−*13*). However, flavonoids can also behave as prooxidant species depending on several factors such as their concentration and the type of free radical source. This prooxidant activity has been especially reported when transition metals are available in the media (*14*, *15*).

Flavonoids' structure is based on the flavan motif, and their classification depends on the presence of various substituents on the rings and the degree of pyrane ring saturation. Quercetin is one of the most representative compounds of this family due to its implication in most of the biological processes cited above. Quercetin presents three structural groups, determinant for its free radical scavenging and/or antioxidative potential: (i) a catechol moiety (B-ring), (ii) a carbonyl function on the C-ring conjugated to two hydroxyl groups on C_3 (C-ring) and C_5 (A-ring), and (iii) a double bond between C_2 and C_3. These hydroxyl groups may be dehydrogenized, deprotonated, or oxidized in the course of these biological mechanisms. Moreover, this highly functionalized structure provides the possibility for a metal cation to interact with the substrate on three complexing sites (see **Figure 1**). However, it seems that this natural product may act, in most of cases, after being metabolically activated (*16*), and despite a constant increase of knowledge on both positive and negative biological effects of quercetin, it remains often unclear which activated form should play a role in a given process.

Indeed, semiquinone and quinone forms of quercetin, deriving from the abstraction of respectively one or two $H^{\bullet}$, are involved in many oxidative processes (*16*−*18*). For instance, quercetin reduces peroxyl radicals involved in lipid peroxidation, and through this reaction, a semiquinone species is produced, which then undergoes a disproportionation to generate a quinone form. Semiquinone and quinone active forms are also directly involved in DNA damage or formation of adducts with amino acids. Alternatively, alkylation of the hydroxyl group located on the A-ring favors inhibition of the Fenton reaction. Oxidation of the catechol moiety via a redox cycle involving Cu^{2+}, O_2, and NADH generates a copper−hydroperoxo complex responsible for oxidative DNA damage. Moreover, transition metal can play a role in both antioxidant and prooxidant processes. Upon binding to the quercetin 2,3-dioxygenase copper center (*19*), a deprotonated quercetin is involved in the metabolisation of dioxygen (*15*, *18*, *20*, *21*).

Quantum chemical computations can in principle provide quantitative predictions of the behavior of organic compounds, such as their chemical reactivity, or their physicochemical properties. Among the broad variety of works concerning

* Author to whom correspondence should be addressed [fax +33 / (0) 4 92 07 61 25; e-mail Serge.Antonczak@unice.fr].

10.1021/jf061864s CCC: $37.00
Published on Web 01/17/2007

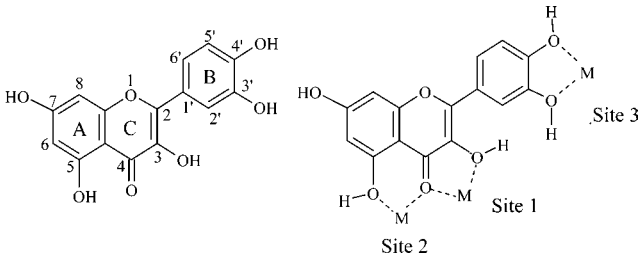

Figure 1. Structure of quercetin and binding sites for metal chelation. Systematic numbering of atoms and cycles are also presented.

flavonoids, only a few theoretical studies focused on the electronic, structural, and energetic properties of quercetin (*22*−*25*). Electronic density is delocalized over the whole structure as shown by theoretical studies handled by van Acker et al. (*24*) and Leopoldini et al. (*25*) at the UHF/6-31G*//UHF/STO-3G and B3LYP/6-31++G** levels of computation, respectively. Zhang et al. (*26*), in a study performed at the B3LYP/6-31G-(d,p) level, have also put forward that the formation of a intramolecular H-bond has an influence on the bond energies. These results were in good agreement with results obtained by Wright et al. (*27*). Recently, Leopoldini et al. have published a paper devoted to calculations of acidity of natural antioxidants, in both gas and liquid phases, performed at the B3LYP/6-311++G** level of computation (*28*). Semiquinone forms have been considered as the central subject of some theoretical works, but discrepancies in the results have been obtained. Indeed, van Acker et al. (*29*) have shown that abstraction of a single hydrogen atom led to atomic spin densities highly localized on the oxygen atom from which the hydrogen was abstracted, whereas Russo et al. (*30*) have put forward that this spin density was delocalized over the neighboring atoms. More recently, in a study devoted to bond energies as well as spin densities of radical structure deriving from quercetin, Trouillas et al. (*31*) have confirmed the importance of the C2−C3 double bond in electron localization. None has tried to rationalize systematically the reactivity of quercetin activated forms. To specify the properties of deprotonated, semiquinone, and quinone forms as well as the influence of copper on their reactivity, each quercetin active form was studied by means of theoretical methods.

THEORETICAL CALCULATIONS

As detailed in a previous study (*32*), B3LYP density functional method (*33*, *34*) using the 6-31G* basis set (*35*) reproduces adequately quercetin crystallographic data (*36*), but an additional diffuse function (+) (*37*−*39*) on the oxygen atom is necessary to obtain a much better description of the system energetics. Addition of diffuse functions on carbon atoms did not improve the quality of the results and was much more time-consuming. LanL2DZ (*40*) Los Alamos ECP has been used to represent the copper atom. It has been verified that such a level of computation is sufficient to represent accurately both charge distributions and charge transfers from the ligand to the metal center. Optimizations have been conducted using the MP2 (*41*) method to assess the validity of the method. Quercetin, as well as a deprotonated and a semiquinone form (denoted, respectively, D1 and SQ1 in the following; see Results and Discussion) have been predicted to be planar by this post-HF method, as found with the B3LYP functional on similar structures, leading us to be confident in the choice of our level of computation. In summary, optimizations have been performed using the Gaussian98 (*42*) program with the B3LYP method and a 6-31G* basis set for C and H atoms, a 6-31+G* basis set for oxygen atoms, and the LanL2DZ potential for the copper atom.

The average effect of the bulk solvent on the structures and properties of the molecules studied throughout this work is examined using the PCM continuum model (*43*). The solute is assumed to be placed into a cavity created in a dielectric continuum. Due to the charge distribution of the solute, the continuum is polarized and creates an electric field inside the cavity that polarizes in return the solute. In these calculations, the dielectric permittivity of the solvent is taken to be 78.4, corresponding to that of bulk water. Structures have been optimized in this framework at the same level of computation [B3LYP/6-31(+)G*] as that used in the gas phase.

Vibrational frequencies of the optimized structures, both in vacuum and in solvent, were computed using the same level of theory, and thermodynamic corrections (*44*), obtained at 298 K and 1 atm, have been added to the electronic energies. Unless noted, reaction enthalpies will be given for proton, hydrogen, or electron abstractions, and reaction free energies will be given when coreactive species are considered. Net atomic charges have been computed using the NBO package of Gaussian98, following the NPA procedure (*45*). When necessary, radical compounds are described with Mulliken atomic spin density. Total spin values $<S^2>$ have been checked for each structure, and no spin contamination has been found.

RESULTS AND DISCUSSION

Quercetin (Q) activated forms can be split into five functionalized groups (see **Figure 2**), namely, semiquinone (SQ), deprotonated (D), double deprotonated (DD), semiquinone deprotonated (SQD), and quinone (OQ). Radical cation species (Qr) was also considered. In the following, the evolution of energetic, structural, and electronic properties of each series, together with the influence of complexation with a metal cation, is presented. Energies reported here for deprotonation and homolytic cleavage of OH function, as well as for reduction processes, may appear large by comparison with reaction energies classically found for biological processes. However, one has to keep in mind that a detailed analysis of these reactions cannot be carried out without considering coreagents.

Activated Forms Computed in the Gas Phase. *D Forms.* Energetic values (ΔH as reported in **Table 1**) obtained according to the $Q \rightarrow D + H^+$ reaction scheme (proton affinity, PA) range from 318.2 to 337.6 kcal mol^{-1} (formation of D5 and D2, respectively). The large PA values found in the case of the formation of D1 and D2 forms are consistent with the subsequent loss of an intramolecular H-bond. The average difference between enthalpy values obtained here with those calculated by Leopoldini et al. (*28*) is about 1 kcal mol^{-1}. These two levels of calculations exhibit the same ranking as well as the same range concerning these enthalpies. From a structural point of view, the deprotonation reaction does not affect geometries drastically. The only noticeable change in bond length consists in a decrease of each C−O bond involved in the proton abstraction and is similar for all five forms (roughly 0.1 Å). The electronic aspect is more interesting. Unexpectedly, the net atomic charges of the oxygen atoms involved in the deprotonation are not modified with respect to the values found in the Q form (-0.07 e $< \Delta qO < +0.01$ e), indicating that the excess of negative charge arising from proton abstraction is distributed over the rings. Two different trends depending on in which atom the proton is abstracted are reported (see **Table 1**). When the deprotonation occurs on O_3, O_5, or O_7, the additional charge is distributed only on atoms of the A-ring, but if deprotonation occurs on O_3' or O_4', an important charge transfer is reported from B to AC conjugated rings (0.20 and 0.31 e for D4 and D5 forms respectively). The highly conjugated π system between A and C neighbor rings is sufficient to explain these differences.

DD Forms. Two different doubly deprotonated quercetin (DD1 and DD2) and two alternative conformers (DD3 and DD4) are considered. These forms can further lead to the semiquinone or *o*-quinone structures that are considered as crucial intermedi-

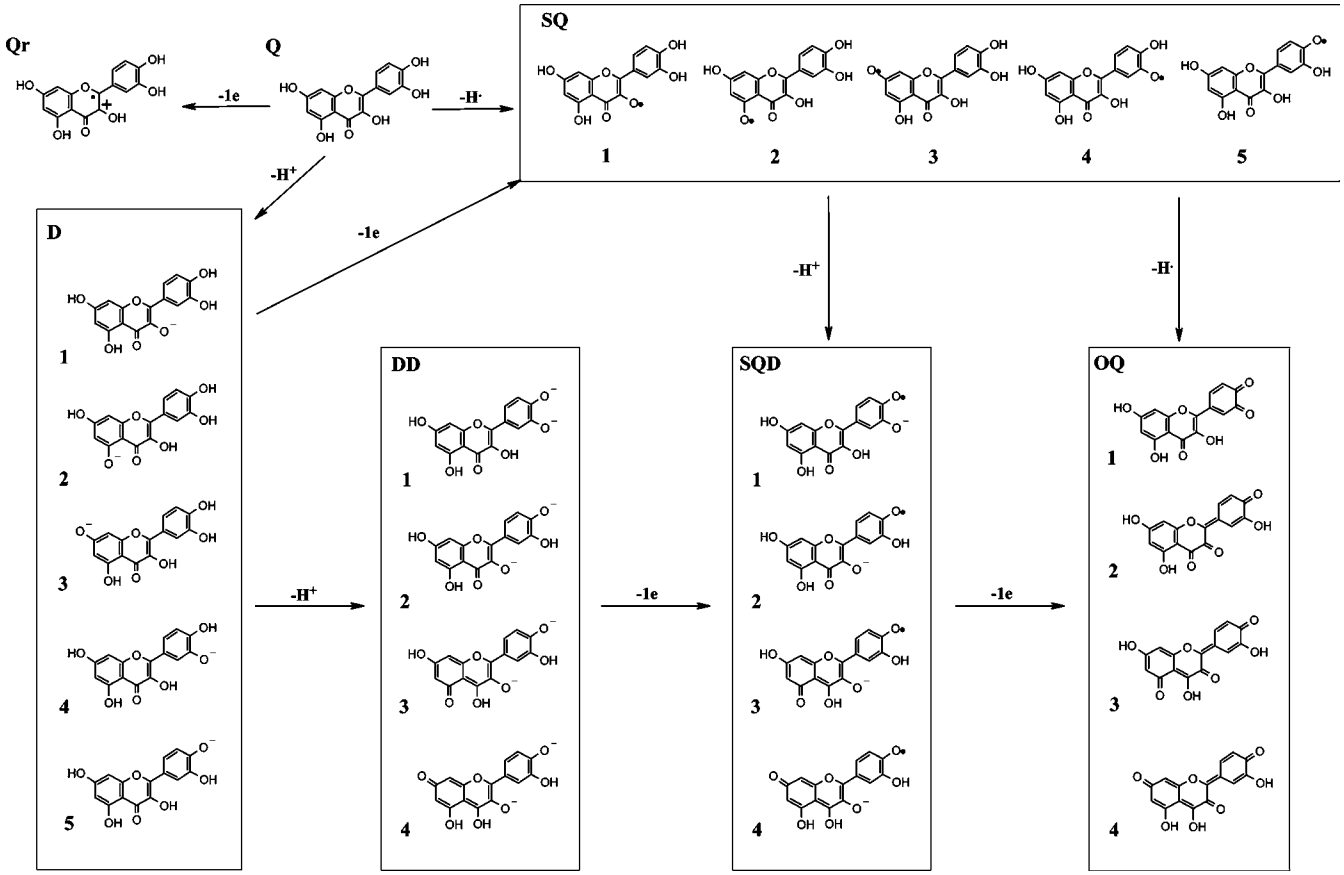

Figure 2. Structure and classification of quercetin active forms. Q, quercetin; Qr, radical quercetin; D, deprotonated forms; SQ, semiquinone forms; DD, double-deprotonated forms; SQD, semiquinone deprotonated forms; OQ, *o*-quinone forms.

Table 1. Reaction Energies (ΔH and ΔG) and Sum of NPA Atomic Charges for Rings A and C (Σq_{AC}) and for Ring B (Σq_B) Computed for Each Structure in the Gas and Solvent Phases

	Q – e		Q → Dx + H+					Q → SQx + H•				
	Qr	Q	D1	D2	D3	D4	D5	SQ1	SQ2	SQ3	SQ4	SQ5
ΔH_{gas} (kcal mol^{-1})	163.1		331.2	338.0	322.6	324.4	317.5	77.1	92.0	83.0	72.5	70.0
ΔG_{gas} (kcal mol^{-1})	163.1		331.6	337.6	322.9	327.0	318.2	68.8	83.0	74.5	64.3	62.1
ΔH_{H2O} (kcal mol^{-1})			290.1	292.3	286.7	289.8	286.3	77.1	87.7	87.4	79.4	76.3
ΔG_{H2O} (kcal mol^{-1})			288.3	292.2	287.2	289.0	285.5	66.2	78.9	77.2	69.2	68.4
electronic distribution												
Σq_{ACgas} (e)	0.51	–0.06	–0.86	–0.94	–0.95	–0.26	–0.37	–0.14	–0.07	–0.12	–0.01	0.03
Σq_{Bgas} (e)	0.49	0.06	–0.14	–0.06	–0.05	–0.74	–0.63	0.14	0.07	0.12	0.01	–0.03
$\Sigma q_{AC,H2O}$ (e)		–0.07	–0.95	–1.02	–1.03	–0.13	–0.22	–0.21	–0.11	–0.20	0.01	0.07
$\Sigma q_{B,H2O}$ (e)		0.07	–0.05	0.02	0.03	–0.87	–0.78	0.21	0.11	0.20	–0.01	–0.07

	D5 → DDx + H+				SQ5 → SQDx + H+				SQ5 → OQx + H•			
	DD1	DD2	DD3	DD4	SQD1	SQD2	SQD3	SQD4	OQ1	OQ2	OQ3	OQ4
ΔH_{gas} (kcal mol^{-1})	422.6	403.4	400.8	391.6	322.3	313.8	316.8	316.2	72.2	69.4	75.9	81.1
ΔG_{gas} (kcal mol^{-1})	421.7	403.3	400.9	392.1	321.9	313.9	317.0	316.4	63.6	61.3	68.1	73.0
ΔH_{H2O} (kcal mol^{-1})	304.2	295.2	298.0	301.3	280.6	278.0	283.2	288.8	73.6	70.9	76.8	83.9
ΔG_{H2O} (kcal mol^{-1})	305.5	295.4	297.7	301.5	280.4	277.4	284.8	287.8	63.7	61.1	69.3	74.0
electronic distribution												
Σq_{ACgas} (e)	–0.79	–1.11	–1.16	–1.19	–0.30	–0.58	–0.61	–0.64	0.05	–0.04	–0.04	0.01
Σq_{Bgas} (e)	–1.21	–0.89	–0.84	–0.81	–0.70	–0.42	–0.39	–0.36	–0.05	0.04	0.04	–0.01
$\Sigma q_{AC,H2O}$ (e)	–0.34	–1.07	–1.13	–1.16	–0.1	–0.56	–0.59	–0.61	–0.11	–0.02	–0.01	–0.02
$\Sigma q_{B,H2O}$ (e)	–1.66	–0.93	–0.87	–0.84	–0.9	–0.44	–0.41	–0.39	0.11	0.02	0.01	0.02

ates for biochemical reactions. The deprotonation of D5 that leads to either DD1 or DD2 is associated with enthalpy values quite similar to the ones found for the first deprotonation (ΔH = 421.7 and 403.3 kcal mol^{-1}, respectively). As expected, it is less favorable to deprotonate a second oxygen on the catechol group rather than on another ring. Moreover, DD3 and DD4 forms are more stable than DD1 and DD2, suggesting that formation of these two forms should be preferential in the biological environment. Structural parameters are not noticeably affected by the second deprotonation. Note, however, a slight decrease of the CO bond distance involved in the proton abstraction ($\Delta d_{C-O} \approx -0.1$ Å).

The electron density initially localized on the hydrogen atom (≈0.5 e in each case) is delocalized on the three rings (see **Table**

Table 2. Energy Values for Dx → SQx and SQDx → OQx Processes in the Gas Phase

	Dx → SQx		SQDx → OQx	
x (kcal mol^{-1})	ΔH	ΔG	ΔH	ΔG
1	58.3 (97.0)[a]	57.8 (96.1)	62.3 (103.0)	62.3 (101.5)
2	66.5 (105.5)	66.0 (104.9)	68.1 (102.9)	68.0 (101.9)
3	72.8 (110.7)	72.2 (108.2)	71.6 (103.7)	71.7 (102.7)
4	60.5 (99.6)	57.9 (98.4)	77.4 (105.1)	77.2 (104.4)
5	64.9 (99.9)	64.5 (101.1)		

[a] In parentheses are given the same value as computed in the solvent phase.

Table 3. Atomic Spin Densities on Pertinent Atoms for Semiquinone (SQ) and Deprotonated Semiquinone (SQD) Structures Computed in the Gas Phase

	SQ1	SQ2	SQ3	SQ4	SQ5	SQD1	SQD2	SQD3	SQD4
C2	0.37	0.03	0.06	0.01	–0.12	0.02	0.03	–0.01	–0.04
C3	0.01	0.05	0.04	0.00	0.17	0.03	0.08	0.08	0.15
C6	0.01	0.36	0.18	0.00	–0.01	0.00	–0.02	–0.01	0.04
C8	0.04	0.45	0.41	0.00	–0.01	0.00	–0.01	0.02	0.09
C10	–0.01	0.17	0.28	0.00	0.00	–0.01	–0.03	–0.02	0.09
C1′	–0.08	–0.01	–0.01	–0.06	0.29	0.01	0.12	0.13	0.15
C2′	0.09	0.01	0.02	0.19	–0.14	0.27	–0.07	–0.07	–0.08
C3′	–0.05	–0.01	–0.01	0.00	0.25	0.02	0.09	0.09	0.10
C4′	0.13	0.02	0.03	0.28	0.01	0.03	0.06	0.05	0.05
C5′	–0.06	0.00	–0.01	–0.14	0.15	0.03	0.06	0.06	0.07
C6′	0.13	0.01	0.03	0.32	–0.07	0.05	0.04	0.02	0.01
O3	0.31	0.02	0.02	0.00	0.04	0.01	0.24	0.25	0.18
O5	0.01	0.33	–0.02	0.00	0.00	0.00	0.01	0.04	0.00
O7	0.00	–0.01	0.39	0.00	0.00	0.00	0.00	0.01	0.10
O3′	0.00	0.00	0.00	0.35	0.07	0.31	0.02	0.02	0.02
O4′	0.03	0.00	0.01	0.08	0.29	0.13	0.17	0.16	0.17

1). The O4′ atomic charge increases by 0.05 e when passing from D5 to DD1, whereas when DD2, DD3, and DD4 are formed, the charge of this atom decreases by ~ -0.08e. The same trend is reported for both C3 and C4′ carbon atoms. In a general manner, abstraction of this second proton leads to a limited electron delocalization between the rings and thus to an enhanced charge density on the cycle where H^+ has been abstracted (see **Table 1**).

SQ Forms. Semiquinone forms are highly reactive species and are obtained through the homolytic hydrogen dissociation of a quercetin (Q → SQ + H$^\bullet$). The two lower enthalpy values ($\Delta H = 70.0$ and 72.5 kcal mol^{-1}) found for hydrogen abstraction on the catechol group are in agreement with experimental considerations, suggesting that the catechol's two hydroxyl groups are highly reactive in the presence of radical species (*46*). Another way to obtain SQ forms consists in the oxidation process (D → SQ + e$^-$) that corresponds to the ionization potential (IP) for each of the deprotonated forms (see **Table 2**). From a structural point of view, abstraction of H^+ or H$^\bullet$ induces about the same geometric variations of the structure (e.g., $\Delta d_{C-O} \approx 0.1$ Å, and $\Delta d_{C-Cvicinal} \approx 0.06$ Å).

Electronic analysis of the resulting structure, especially concerning the localization of the unpaired electron (see **Table 3**), has revealed that for the five SQ forms, >93% of the unpaired electron is localized on about four atoms, including the oxygen from which H$^\bullet$ has been abstracted. Two different trends are reported. The atomic spin densities remain localized on the A-ring when SQ2 and SQ3 are concerned and on the B-ring when SQ4 is concerned. When H$^\bullet$ is abstracted either on O3 or on O4′, the atomic spin density is delocalized over the two B- and C-rings. In all of the cases, these results are in good agreement with the tautomer forms that can be written following the Lewis formalism. The influence of an external factor, such as the approach of a coreactive species close to one of these positions, can lead to an increase of these electron densities on a clearly defined atom and thus leads to an enhanced reactivity of a specific position. These results emphasized the broad variety of reactivity of these semiquinone structures.

Table 4. Energy Values for Coreactive Species Reactions

	reaction	ΔH (kcal mol^{-1})	ΔG (kcal mol^{-1})
+ e	$H^+ \rightarrow H^\bullet$	–312.4	–320.6
	$OH \rightarrow OH^-$	–39.6	–39.2
	$O_2 \rightarrow O_2^{-\bullet}$	–14.3	–14.2
	$HOO \rightarrow HOO^-$	–23.3	–23.1
	$HCOO \rightarrow HCOO^-$	–78.4	–77.5
	$Cu^{+2} \rightarrow Cu^+$	–479.6	–479.2
+ H^+	$OH^- \rightarrow H_2O$	–384.4	–385.6
	$O2^{-\bullet} \rightarrow HOO^\bullet$	–344.5	–346.3
	$HOO^- \rightarrow H_2O_2$	–368.7	–368.7
	$HCOO^- \rightarrow HCOOH$	–337.4	–338.1
+ H$^\bullet$	$OH \rightarrow H_2O$	–111.6	–104.2
	$HOO \rightarrow H_2O_2$	–79.5	–71.2
	$HCOO \rightarrow HCOOH$	–103.3	–95.0
	$O_2 \rightarrow HOO^\bullet$	–46.3	–39.9
	$O_2^{\bullet-} \rightarrow HOO^-$	–55.4	–48.8

It would be illusory to try to rationalize the reactivity of quercetin actived forms without taking into account the coreactive species involved in the various antioxidant and antiradical processes. To this end, free energies associated with proton, electron, or hydrogen abstraction from quercetin (**Tables 1** and **2**) will be compared to free energies associated with theses coreactions (see **Table 4**). These data, analyzed within the framework of thermodynamic cycles as shown in **Figure 3**, are extremely useful to understand which way may be the most favorable.

As exposed in **Figure 3a**, three ways may be considered for the formation of SQ5 semiquinone form. Then, for both Q → Qr → SQ5 and Q → D5 → SQ5 reaction schemes, the abstracted electron can be used to reduce OH$^\bullet$ into OH^- and the abstracted proton can react with OH^- to produce H_2O. In the direct reaction, namely, Q → SQ5, it is assumed that OH$^\bullet$ will directly react with H$^\bullet$. In the three cases, the overall free energy is -42.0 kcal mol^{-1}. The first and second steps of the Q → Qr → SQ5 scheme are associated with energy values of $\Delta G = 124.0$ and -166.0 kcal mol^{-1}, respectively. Concerning the Q → D5 → SQ5 reaction scheme, the first and second steps are associated with energy values of $\Delta G = -67.3$ and 25.3 kcal mol^{-1}, respectively. Thus, it can be concluded that OH$^\bullet$ is not a reducing agent strong enough for the first reaction scheme to be considered because the first step is too energetically demanding. By considering different coreactive species, such as O_2, that could be reduced by electron transfer into $O_2^{\bullet-}$, or $HCOO^-$ that could be neutralized by H^+ into HCOOH (formic acid is often used as a model for glutamate and aspartate side-chains), one obtains the same trends. The first reaction scheme is associated with respectively, $\Delta G = 149.0$ and -118.5 kcal mol^{-1} for the two successive steps and the second one with energy values of $\Delta G = -19.8$ and 50.3 kcal mol^{-1}. It appears then clearly that a good reducing agent favors the former process. However, analysis of the sole deprotonation, homolytic cleavage, and reduction processes would have led to completely different rankings, and thus energies reported here will help in rationalizing most of the mechanism propositions.

SQD Forms. Formation of deprotonated semiquinones can proceed through three different pathways: abstraction of H$^\bullet$,

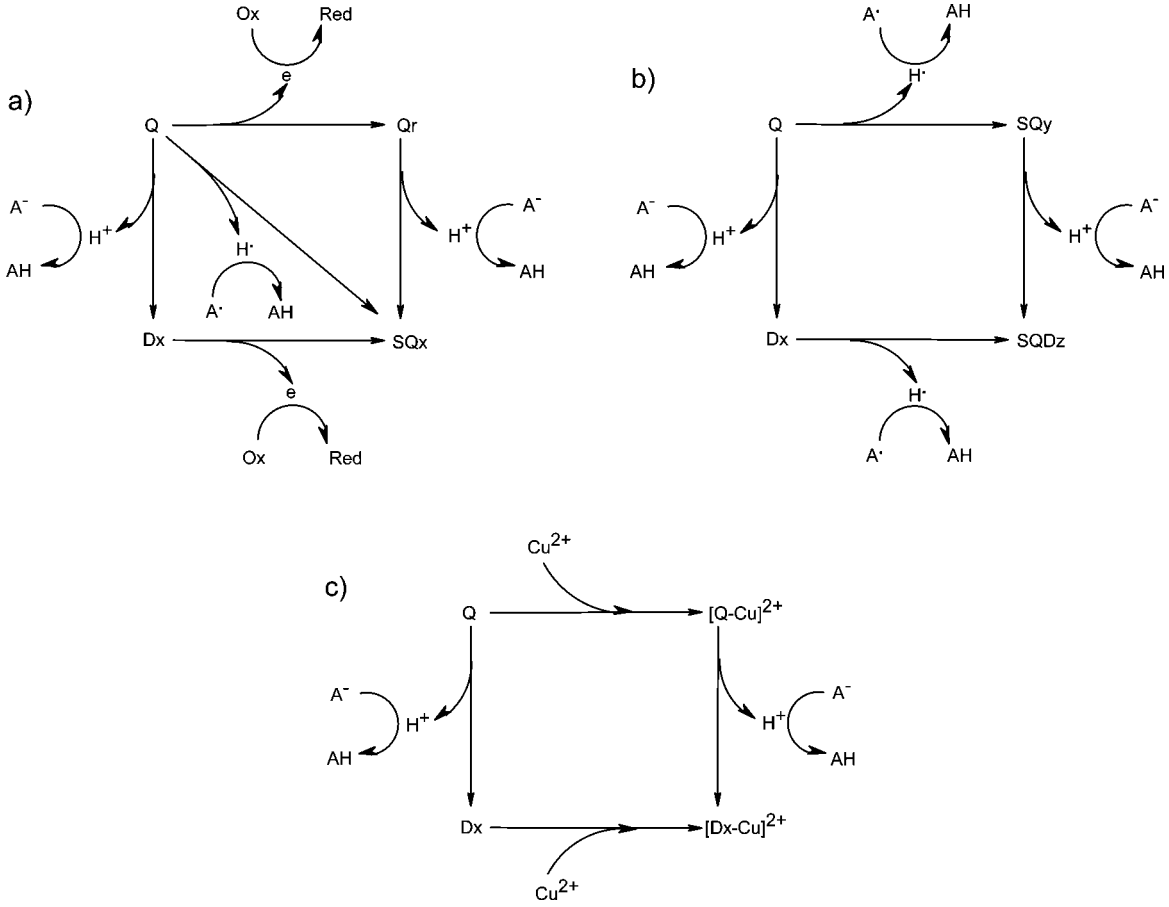

Figure 3. Thermodynamic cycles in which quercetin activated forms could be involved.

H^+, or an electron from D, SQ, or DD forms, respectively. Considering the most stable deprotonated form, that is, D5, the BDE are in the range of $\Delta H = 66.2$ and 74.8 kcal mol^{-1}. Considering the most stable semiquinone form, that is, SQ5, the PA values lie between $\Delta H = 313.9$ and 321.9 kcal mol^{-1}. Considering the DDx → SQDx scheme, low ionization potentials in the range of $\Delta H = 10.6$ and 35.4 kcal mol^{-1} are found. The SQD and DD forms are very similar from a structural point of view (bond length differences lower than 0.04 Å). SQD2, SQD3, and SQD4 are energetically very similar ($\Delta G < 3.1$ kcal mol^{-1}), whereas SQD1 is 8.0 kcal mol^{-1} higher in energy than the most stable SQD2.

Let us consider a thermodynamic cycle, as shown in **Figure 3b**, to compare the free energies associated with the production of SQD2, for instance. $HOO^\bullet$ and OH^- may be considered as the coreactive species that could react, respectively, with $H^\bullet$ and H^+. The free energies for the two successive steps of the Q → SQ5 → SQD2 reaction scheme are $\Delta G = -9.1$ and -71.7 kcal mol^{-1}, respectively, whereas the values for the two successive steps of the Q → D5 → SQD2 reaction scheme are $\Delta G = -67.4$ and -13.4 kcal mol^{-1}, respectively. Whatever the selected way, production of SQD2 is energetically favored, but if it is estimated that the first step (consisting of the activation of the initial quercetin) is the most important, then the second reaction scheme could be considered as the most probable. On this basis, the use of HOO^- and $OH^\bullet$ as the coreactive species leads then to comparable values for the two steps of the two processes that cannot allow discrimination between the two reaction schemes. Indeed, in this case, the free energies for the two successive steps of the Q → SQ5 → SQD2 reaction scheme are $\Delta G = -42.0$ and -54.9 kcal mol^{-1}, respectively, whereas the values for the two successive steps of the Q → D5 → SQD2 reaction scheme are $\Delta G = -50.5$ and -46.4 kcal mol^{-1}, respectively.

This type of analysis can also be used in the case of the SQD1 formation by the lactoperoxidase enzyme, as reported experimentally (*16*). The formation of the free radical intermediate occurs during the LPO-catalyzed oxidation of quercetin according to the classical peroxidase mechanism $2Q + H_2O_2 \rightarrow 2SQD1 + 2H_2O$. Here, energetics favor transition through the D4 form, but these relative energies may be modulated by changing the molecular entity that captures H^+ from quercetin. The $H^\bullet$ abstraction is influenced by the overall charge of the molecule, and it is clear that the negative charge facilitates the homolytic cleavage.

The specific reactivity of these SQDx radicals can partly be rationalized by inspecting atomic spin densities for each structure (see **Table 3**). As expected, SQD2, SQD3, and SQD4 show that the unpaired electron is located partly on O_3 and O_4' and on their vicinal carbon atoms, proving here that the delocalization of the unpaired electron is effective between AC- and B-rings. Moreover, inspection of the charge fluctuations between SQ and SQD forms puts forward that O_3, for these three forms, loses ≈0.1 electron, whereas O_4 gains ≈0.1 electron (the remaining 0.3 e being delocalized over the rings). In contrast, for SQD1, spin density is mainly localized on the three C_2', O_3', and O_4' atoms, whereas the excess of electrons brought by the abstraction of the H^+ is delocalized over the rings. These findings suggest that SQD structures are likely to lose an additional electron to lead to *o*-quinone forms. These results support the high reactivity of the *o*-semiquinone ($Q^{\bullet -}$) reported by Metodiewa et al. (*16*).

OQ Forms. Quinone forms are often considered as stable intermediates produced in the course of the biochemical transformation or metabolization of flavonoids, as reflected by numerous publications on the subject (*47*−*49*). In the present study, they are considered as the final product of successive oxidation and/or deprotonation processes. Two major pathways lead to the stable quinone forms (OQ): abstraction of an electron or of H•, respectively, from SQD or SQ structures. Energetics for these two ways (see **Tables 1** and **2**) show that they are not energetically too different. However, on the basis of their relative stabilities, quinone can be divided into two groups: OQ1 and OQ2 versus OQ3 and OQ4. The fact that the C_4O_4 carbonyl group and the aromaticity of the A-ring are preserved on OQ1 and OQ2 could explain this statement. Geometry analysis confirms the formal single, double, and aromatic bonds presented in **Figure 1**. In addition, the most important difference between Q and OQ form atomic charges is located on the oxygen and carbon atoms involved in the formation of the carbonyl group.

Activated Forms Computed in the Solvent Phase. Although gas phase predictions are appropriate for many purposes, they are inadequate for describing the characteristics of polar and/or charged molecules placed in a solvent with high dielectric constant. To model this solvent effect from both a structural and energetic point of view, quercetin activated forms have been optimized in a dielectric continuum using SCRF-PCM methodology. Note that, in a protein cavity, the electric field cannot be simply reproduced by a dielectric continuum because the environment is not isotropic in each direction around the substrate. Moreover, by polarization effects, neighboring amino acids play a particular role in the recognition/activation processes of the substrate. However, in a first approach, the reaction field produced by an entire protein can be reproduced in a primary approximation by a dielectric continuum with a low dielectric permittivity value. Here, on the basis of these considerations and since the use of the thermodynamic cycles is meant to be an aid for rationalizing the influence of a coreactive species, no such analysis implying coreactive species will be considered in this section.

Generally speaking, the absolute energies for each form are lowered when placed in the solvent, enhancing the fact that these activated forms bear highly polarizable functions. Furthermore, it appears that the absolute energies of activated forms in a given series (deprotonated, semiquinone, and double deprotonated) are closer to each other when computed in the solvent with respect to vacuum. This is not the case for both deprotonated semiquinones and quinones, for which the differences between the absolute energy of the most and the less stable compounds are quite similar either in solvent or in vacuum.

D Forms. On average, proton affinities (see **Table 1**) are lowered when computed in bulk water by about 37.7 and 39.0 kcal mol^{-1} in terms of ΔH and ΔG, respectively. The ranking of the deprotonation energies is not modified with respect to the results obtained in the gas phase, and here again, it remains easier to deprotonate quercetin in the O4′ position. Leopoldini et al. (*28*) have performed such proton affinity calculations in water, and their results also put forward that the absolute energies of the deprotonated forms are closer to each other when computed in the solvent with respect to vacuum. The energy range they obtained is in good agreement with the one obtained here. Nevertheless, the ranking they obtained is modified with respect to gas phase calculations, and the authors have shown that, in the liquid phase, it is easier to deprotonate the O7 oxygen atom. Generally speaking, no drastic evolution of the atomic charge distribution is noticed except for the charge handled by the oxygen atom from which the proton is abstracted, which is more negative by 0.10−0.13 e. The solvent leads, as expected, to a higher charge separation, but this charge evolution is delocalized on the whole structure and not only on the surrounding atoms. Nevertheless, this leads to a more localized negative charge on either AC- or B-rings depending on the location of the proton abstraction (O3, O5, and O7 in the first case vs O3′ and O4′ in the second). This result enhances the relative independence of the AC- and B-rings as already put forward in the gas phase. No major change is observed concerning interatomic distances.

DD Forms. The same trends as found for the deprotonated forms can be put forward in this section. The second proton affinities are lowered in average value by roughly 109 kcal mol^{-1}, confirming the stabilization role of the polar solvent on these charged forms. The four energy values corresponding to this second deprotonation are now very close to each other. DD2 and DD1 forms are now, respectively, the most and the least stable structures among this series. Only the oxygen atoms implied in this second proton abstraction are noticeably affected in terms of atomic charges, and inspection of the charge repartition over the rings shows minor differences with respect to results obtained in the gas phase, except for DD1. In solvent, the B-ring is able to accept additional an 0.45 e. Considering this point and the important decrease in deprotonation energy of this form, it can now be considered that this doubly deprotonated form may play an important role in biological processes. Concerning interatomic distances, no major change is observed.

SQ Forms. In this series, whereas the ranking in energy is not highly modified on going from the gas phase to the solvent phase, the hydrogen abstraction energetics are nonetheless smaller in the condensed phase. On average, it remains slightly easier to abstract the hydrogen in the gas phase. When the formation of these semiquinones forms is considered from the corresponding deprotonated structures (see **Table 2**), it appears that the associated energies are noticeably higher than in the gas phase. This comes from the important stabilization of the D structures when optimized in the continuum that is partly lost by abstraction of an electron. No noticeable modifications are reported either for the atomic charges, interatomic distances, or atomic spin densities.

SQD Forms. Here, proton abstraction related to deprotonated semiquinone formation from semiquinone forms is lowered when computed in bulk water by about 37 kcal mol^{-1} in terms of ΔH or ΔG. The ranking is modified, and due to a high destabilization of SQD4 with respect to SQD1, the energy range is larger when the solvent is taken into account. Because this process is similar to the one leading to the formation of the deprotonated form, the same tendencies in terms of charge distributions are found for the present forms.

OQ Forms. Abstraction of a hydrogen atom from the SQ5 form leads to the same trends as those found for the same processes leading to SQ activated structures. Enthalpies related to the process are comparable in the gas and condensed phases, although absolute energies reveal a stabilization of the structures when computed with the continuum model. The ranges of energies are similar, and the ranking is identical. It remains, however, slightly favorable to form the quinone structures in the gas phase. As put forward in the case of semiquinone series, the formation of the present structures from a charged species (SQDx, see **Table 2**) is energetically more demanding in water, due to the loss of an entire charge on the molecule. Here again,

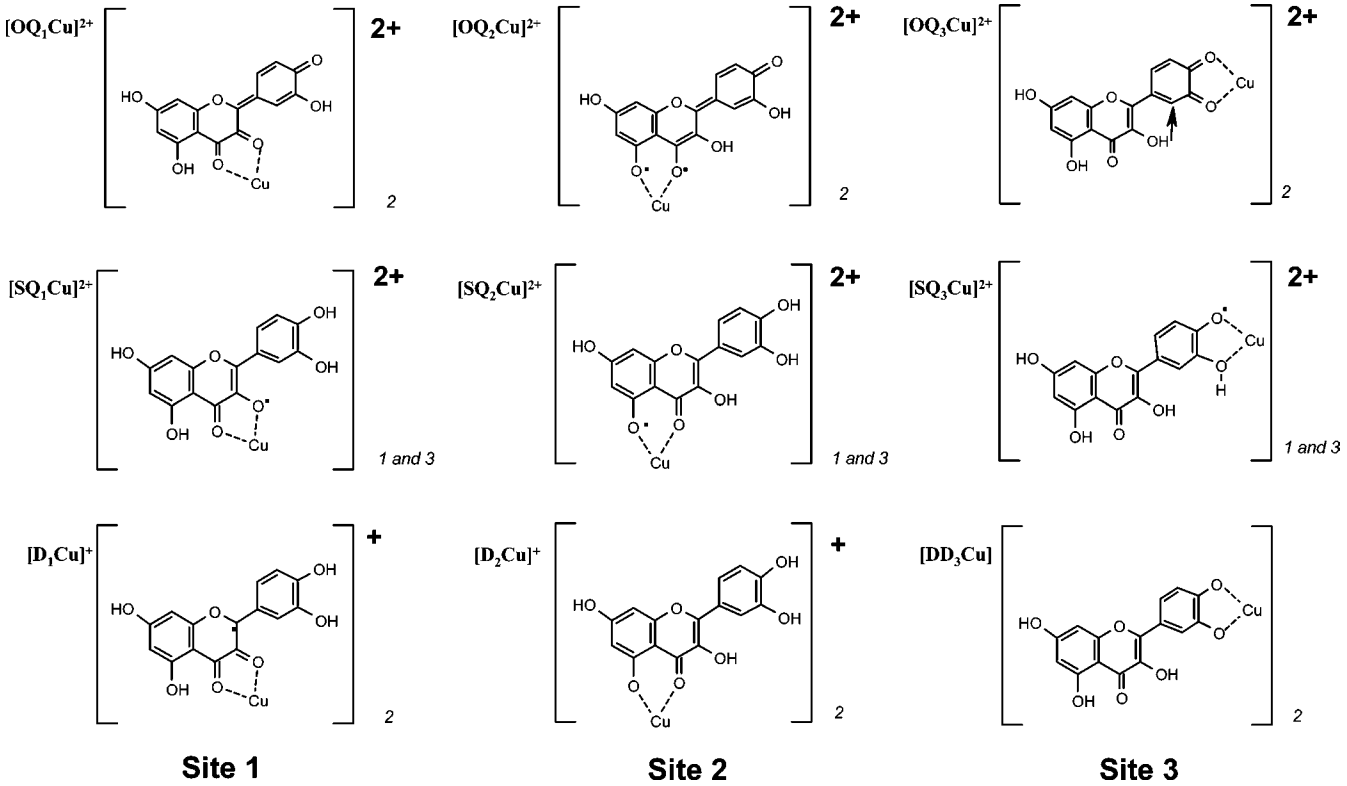

Figure 4. Structure and classification of quercetin active forms complexed with a copper(II) ion. At the bottom of each structure is given the spin multiplicity considered (see also **Table 5**).

no important evolutions are reported concerning atomic charges, spin densities, and interatomic distances.

Generally speaking, a polar solvent facilitates the formation of the charged species and shows only slight influences on the formation of the radical structures by proton abstraction but important energetic increase by electron abstraction. Thus, one may imagine that the use of thermodynamic cycles compatible with reactions undertaken in water could give completely different energetic previsions.

Quercetin Activated Forms Complexed with a Metal Ion (Gas Phase). Quercetin structure gives the opportunity for metal cations to bind on three different sites, either on 3-hydroxychromone or on 5 hydroxychromone functions or on hydroxyl groups of the catechol moiety (denoted sites 1, 2, and 3, respectively). Iron or copper atoms are the metal centers most often involved in biological processes in which quercetin plays a critical role either as antioxidant, prooxidant, or inhibiting substance. Here copper has been chosen because in most of the processes proposed in the literature, quinone, semiquinone, and deprotonated quercetin bind a copper(II) cation. Moreover, this metal center plays a central role in dioxygen metabolization by quercetin (*32*). In **Figure 4** are shown the nine complexes formed by complexation with Cu^{2+}. Each of the complexes, except $[OQ_3Cu]^{2+}$, is derived from the uncomplexed species analyzed above.

Complexation does not lead to drastic evolution of the structural parameters as reflected by the slight bond length evolutions (roughly ±0.1 Å). Electronic analysis shows that the charge on the copper center is in the range of 0.91−0.98 e except when complexed to a double-deprotonated quercetin ($q_{Cu} = 0.86$ e), suggesting that quercetin is oxidized whatever the starting form. These findings show that even radical forms such as SQ are likely to be oxidized. This electron transfer is always slightly higher on site 1 or 3 than on site 2. A constant zero value of the copper atomic spin density indicates an electronic transfer from quercetin to copper for all six complexes. Spin densities for the other atoms are very different if the copper is complexed on site 1, 2, or 3, but a general tendency shows a distribution of the unpaired electron essentially on C_8 (20−50% of the spin density) except for D_1Cu and DD_3Cu complexes. Finally, a lowering of the atomic charges occurs on oxygen atoms involved in the complexation with the metal ion. The electronic transfer is slightly higher in the case of a deprotonated form (≈1.2 e) than in the case of the semiquinone one (≈1.1 e). The same increase is observed from the quinone form to the semiquinone one. In the case of the SQ forms, sites 1 and 2 present a better complexation energy than site 3. In the case of the OQ forms, the binding sites are classified as 2 > 3 > 1.

As expected, complexation of Cu^{2+} on each of the quercetin activated forms is favorable, as reflected by the important stabilizing energies for these processes (see **Table 5**), but more interesting are the consequences of these complexations. First,

Table 5. Complexation Energies of Quercetin Activated Forms with Cu^{2+}

complexed species	initial activated form	ΔG of complexation (kcal mol^{-1})
OQ1Cu	OQ2	−302.7
OQ2Cu	OQ3[a]	−336.1
OQ3Cu	OQ1	−308.2
SQ1Cu	SQ1	−322.8 (−312.5)[b]
SQ2Cu	SQ2	−323.3 (−328.8)[b]
SQ3Cu	SQ5	−302.7 (−301.5)[b]
D1Cu	D1	−500.2
D2Cu	D2	−499.8
DD3Cu	*c*	−676.7

[a] In OQ3, the hydrogen atom linked to O4 has migrated on O3. [b] Values not in parentheses were obtained for spin multiplicities of 1, and those in parentheses were obtained for spin multiplicities of 3. [c] DD3Cu originates in the double deprotonation on the catechol group.

let us analyze what should be the energetics associated with the Q → Qr → SQ5 reaction scheme (see **Figure 3a**), where Cu^{2+} gains the electron abstracted from Q and OH^- reacts with the proton abstracted from Qr. For the first step, one obtains $\Delta G = -316.1$ kcal mol^{-1}, and the total process is then associated with a ΔG of -482.1 kcal mol^{-1}. Introduction of a highly oxidizing substance, such as a metal cation, in these schemes then strongly favors the formation of quercetin activated forms.

Moreover, complexation of quercetin and its derived activated forms modifies in an important manner their energetics. Take as an example the formation of $[D5\text{-}Cu]^+$ following **Figure 3c**, where the entity which reacts with H^+ is $HCOO^-$. The overall free energy is -495.9 kcal mol^{-1}, which can be decomposed into -305.1 and -190.8 kcal mol^{-1} for the two successive steps of the Q → $[QCu]^+$ → $[D5\text{-}Cu]^+$ scheme and into -19.8 and -476.1 kcal mol^{-1} for the two successive steps of the Q → D5 → $[D5\text{-}Cu]^+$ scheme. As expected, abstraction of a proton from a positively charged species is easier, but, here, it is shown that this abstraction is facilitated by roughly 171 kcal mol^{-1} (i.e., more than half of the total deprotonation energy). Contrarily to most of the mechanisms proposed (*47*), this result puts forward that chelation to a metal should happen prior to deprotonation or $H^\bullet$ abstraction. The same trend is obtained concerning the oxygenolysis reaction in quercetin 2,3-dioxygenase, where, on the basis of our results, complexation to the metal is followed by O3 deprotonation (ΔG deprotonation = 147.3 kcal mol^{-1}) rather than the opposite (ΔG deprotonation = 318.2 kcal mol^{-1}).

From these results, it appears clearly that metal cations may act as activators leading to flavonoid activated forms showing higher reactivity toward oxidant or radicals species as stated experimentally (*48*, *50*). Moreover, it has been suggested that flavonoids in general would have a double synergistic action by activating the metal center on which they are bound while having the ability to scavenge superoxide radicals (*51*).

In summary, we have shown in this work that quantum chemical computations can provide quantitative predictions of the behavior of flavonoids activated forms, such as their chemical reactivity or their physicochemical properties. These calculations have brought a new viewpoint on the structural, electronic, and energetic characteristics of each of these families and thus have allowed their reactivity to be delimited.

To some extent, quercetin reactive sites are independent of each other. Indeed, although the planar structure of quercetin induces the idea that electronic delocalization may occur over the whole structure, our results have shown that hydrogen, proton, or electron abstractions lead to limited electron delocalization and thus only to weak structural modifications. These localized atomic spin densities explain the high reactivity of the radical and charged forms deriving from quercetin structure. Solvent effect computations have shown the importance of the surrounding upon energetics associated with the formation of the numerous activated forms deriving from the initial quercetin structure. Going from gas to solvent phase, evolutions of structural parameters as well as electronic distribution remain nonetheless limited.

Then, the use of thermodynamic cycles is of a great help to determine, on the basis of energetics, the most likely processes that may occur when coreactive species are taken into account. Moreover, in a biological medium, numerous factors play a role in the feasibility of organic compounds. For example, our analysis does not take into account direct polarization by surrounding amino acids. The height of activation barriers, which can be calculated only within the framework of the detailed description of a mechanism, is also not present. Nevertheless, such analysis is a good starting point to design some new propositions for biological mechanisms. Thus, we are confident in the fact that such a theoretical approach provides another hint to clarify which reaction is likely to occur among the broad range of quercetin biological activities.

ACKNOWLEDGMENT

CMIM (Centre de Modélisation et d'Imagerie Moléculaire) of the University of Nice and CINES (Centre Informatique National de l'Enseignement Supérieur) are greatly acknowledged for provision of computation time.

LITERATURE CITED

(1) Peterson, J.; Dwyer, J. Flavonoids: dietary occurrence and biochemical activity. *Nutr. Res.* **1998**, *18*, 1995−2018.
(2) Manach, C.; Scalbert, A.; Morand, C.; Remesy, C.; Jimenez, L. Polyphenols: food sources and bioavailability. *Am. J. Clin. Nutr.* **2004**, *79*, 727−747.
(3) Scalbert, A.; Williamson, G. Dietary intake and bioavailability of polyphenols. *J. Nutr.* **2000**, *130*, 2073S−2085S.
(4) Aherne, S. A.; O'Brien, N. M. Dietary flavonols: chemistry, food content, and metabolism. *Nutrition* **2002**, *18*, 75−81.
(5) Hudec, J.; Bakos, D.; Mravec, D.; Kobida, L.; Burdovaä, M.; Turianica, I.; Hlusek, J. Content of phenolic compounds and free polyamines in black chokeberry (*Aronia melanocarpa*) after application of polyamine biosynthesis regulators. *J. Agric. Food Chem.* **2006**, *54*, 3625−3628.
(6) Espinosa-Alonso, L. G.; Lygin, A.; Windholm, J. M.; Valverde, M. E.; Parades-Lopez, O. Polyphenols in wild and weedy Mexican common beans (*Phaseolus vulgaris* L.). *J. Agric. Food Chem.* **2006**, *54*, 4436−4444.
(7) Rochfort, S. J.; Imsic, M.; Jones, R.; Trenerry, V. C.; Tomkins, B. Characterization of flavonol conjugates in immature leaves of pak choi [*Brassica rapa* L. Ssp. *chinensis* L. (Hanelt.)] by HPLC-DAD and LC-MS/MS. *J. Agric. Food Chem.* **2006**, *54*, 4855−4860.
(8) Formica, J. V.; Regelson, W. Review of the biology of quercetin and related bioflavonoids. *Food Chem. Toxicol.* **1995**, *33* (12), 1061−1080.
(9) Havsteen, B. H. The biochemistry and medical significance of the flavonoids. *Pharmacol. Ther.* **2002**, *96*, 67−202.
(10) Di Carlo, G.; Mascolo, N.; Izzo, A. A.; Capasso, F. Flavonoids: old and new aspects of a class of natural therapeutic drugs. *Life Sci.* **1999**, *65*, 337−353.
(11) Cotelle, N. Role of flavonoids in oxidative stress. *Curr. Top. Med. Chem* **2001**, *1*, 569−590.
(12) Jovanovic, S. V.; Steenken, S.; Tosic, M.; Marjanovic, B.; Simic, M. G. Flavonoids as antioxidants. *J. Am. Chem. Soc.* **1994**, *116*, 4846−4851.
(13) Nagao, A.; Seki, M.; Kobayashi, H. Inhibition of xanthine oxidase by flavonoids. *Biosci., Biotechnol., Biochem.* **1999**, *63*, 1787−1790.
(14) Cao, G.; Sofic, E.; Prior, R. L. Antioxidant and prooxidant behavior of flavonoids: structure−activity relationships. *Free Radical Biol. Med.* **1997**, *22*, 749−760.
(15) Yamashita, N.; Tanemura, H.; Kawanishi, S. Mechanism of oxidative DNA damage induced by quercetin in the presence of Cu(II). *Mutat. Res.* **1999**, *425*, 107−123.
(16) Metodiewa, D.; Jaiswal, A. K.; Cenas, N.; Dickancaité, E.; Segura-Aguilar, J. Quercetin may act as a cytotoxic prooxidant after its metabolic activation to semiquinone and quinoidal product. *Free Radical Biol. Med.* **1999**, *26*, 107−116.
(17) Gliszczynska-Swiglo, A.; van der Woude, H.; de Haan, L.; Tyrakowska, B.; Aatrs, J. M. M. J. G.; Rietjens, I. M. C. M. The role of quinone reductase (NQO1) and quinone chemistry in quercetin cytotoxicity. *Toxicol. in Vitro* **2003**, *17*, 423−431.

(18) Hirakawa, K.; Oikawa, S.; Hiraku, Y.; Hirosawa, I.; Kawanishi, S. Catechol and hydroquinone have different redox properties responsible for their differential DNA-damaging ability. *Chem. Res. Toxicol.* **2002**, *15*, 76−82.

(19) Fusetti, F.; Schröter, K. H.; Steiner, R. A.; van Noort, P. I.; Pijning, T.; Rozeboom, H. J.; Kalk, K. H.; Egmond, M. R.; Dijkstra, B. W. Crystal structure of the copper-containing quercetin 2,3-dioxygenase from *Aspergillus japonicus*. *Structure* **2002**, *10*, 259−268.

(20) Steiner, R. A.; Kalk, K. H.; Dijkstra, B. W. Anaerobic enzyme•substrate structures provide insight into the reaction mechanism of the copper-dependent quercetin 2,3-dioxygenase. *Proc. Natl. Acad. Sci. U.S.A.* **2002**, *99*, 16625−16630.

(21) Oikawa, S.; Hirosawa, I.; Hirakawa, K.; Kawanishi, S. Site specificity and mechanism of oxidative DNA damage induced by carcinogenic catechol. *Carcinogenesis* **2002**, *22*, 1239−1245.

(22) Vasilescu, D.; Girma, R. Quantum molecular modeling of quercetin−simulation of the interaction with the free radical t-BuOO. *Int. J. Quantum Chem.* **2002**, *90*, 888−902.

(23) Cornard, J. P.; Merlin, M. J.; Boudet, A. C.; Vrielynck, L. Structural study of quercetin by vibrational and electronic spectroscopies combined with semiempirical calculations. *BIOspektrum* **1997**, *3*, 183−193.

(24) van Acker, S. A. B. E.; de Groot, M. J.; van den Berg, D.-J.; Tromp, M. N. J. L.; Donné-Op den Kelder, G.; van der Vijgh, W. J. F.; Bast, A. A quantum chemical explanation of the antioxidant activity of flavonoids. *Chem. Res. Toxicol.* **1996**, *9*, 1305−1312.

(25) Leopoldini, M.; Marino, T.; Russo, N.; Toscano, M. Density functional computations of the energetic and spectroscopic parameters of quercetin and its radicals in the gas phase and in solvent. *Theor. Chem. Acc.* **2004**, *111*, 210−216.

(26) Zhang, H.-Y.; Sun, Y.-M.; Wang, X.-L. Substituent effects on O-H bond dissociation enthalpies and ionization potentials of catechols: a DFT study and its implications in the rational design of phenolic antioxidants and elucidation of structure-activity relationships for flavonoid antioxidants. *Chem. Eur. J.* **2003**, *9*, 502−508.

(27) Wright, J. S.; Johnson, E. R.; DiLabio, G. A. Predicting the activity of phenolic antioxidants: theoretical method, analysis of substituent effects, and application to major families of antioxidants. *J. Am. Chem. Soc.* **2001**, *123*, 1173−1183.

(28) Leopoldini, M.; Russo, N.; Toscano, M. Gas and liquid phase acidity of natural antioxidants. *J. Agric. Food Chem.* **2006**, *54*, 3078−3085.

(29) Van Acker, S. A. B. E.; van den Berg, D.-J.; Tromp, M. N. J. L.; Griffioen, D. H.; van Bennekom, W. P.; van der Vijgh, W. J. F.; Bast, A. Structural aspects of antioxidant activity of flavonoids. *Free Radical Biol. Med.* **1996**, *20*, 331−342.

(30) Russo, N.; Toscano, M.; Uccella, N. Semiempirical molecular modeling into quercetin reactive site: structural, conformational, and electronic features. *J. Agric. Food Chem.* **2000**, *48*, 3232−3237.

(31) Trouillas, P.; Marsal, P.; Siri, D.; Lazzaroni, R.; Duroux, J.-L. A DFT study of the reactivity of OH groups in quercetin and taxifolin antioxydants: The specificity of the 3-OH site. *Food Chem.* **2006**, *97*, 679−688.

(32) Fiorucci, S.; Golebiowski, J.; Cabrol-Bass, D.; Antonczak, S. Oxygenolysis of flavonoid compounds: DFT description of the mechanism for quercetin. *ChemPhysChem* **2004**, *5*, 1726−1733.

(33) Becke, A. D. Density−functional thermochemistry. III. The role of exact exchange. *J. Chem. Phys.* **1993**, *98*, 5648−5652.

(34) Lee, C.; Yang, W.; Parr, R. G. Development of the Colle−Salvetti correlation-energy formula into a functional of the electron density. *Phys. Rev. B* **1998**, *37*, 785−789.

(35) Hariharan, P. C.; Pople, J. A. The influence of polarization functions on molecular orbital hydrogenation energies. *Theor. Chim. Acta* **1973**, *28*, 213−218.

(36) Jin, G.; Yamagata, Y.; Tomita, K. Structure of quercetin dihydrate. *Acta Crystallogr. C* **1990**, *46*, 310−313.

(37) Clark, T.; Chandrasekhar, J.; Schleyer, P. v. R. Efficient diffuse function-augmented basis sets for anion calculations. III. The 3-21+G basis set for first-row elements, Li-F. *J. Comput. Chem.* **1983**, *4*, 294−301.

(38) Krishnan, R.; Binkley, J. S.; Seeger, R.; Pople, J. A. Self-consistent molecular orbital methods. XX. A basis set for correlated wave functions. *J. Chem. Phys.* **1980**, *72*, 650−654.

(39) Gill, P. M. W.; Johnson, B. G.; Pople, J. A. The performance of the Becke−Lee−Yang−Parr (B-LYP) density functional theory with various basis sets. *Chem. Phys. Lett.* **1992**, *197*, 499−505.

(40) Hay, P. J.; Wadt, W. R. *Ab initio* effective core potentials for molecular calculations. Potentials for K to Au including the outermost core orbitals. *J. Chem. Phys.* **1985**, *82*, 299−310.

(41) Møller, C.; Plesset, M. S. Note on an approximation treatment for many-electron systems. *Phys. Rev.* **1934**, *46*, 618−622.

(42) Frisch, M. J.; Trucks, G. W.; Schlegel, H. B.; Scuseria, G. E.; Robb, M. A.; Cheeseman, J. R.; J. R. Zakrzewski, J. R.; Montgomery, J. A., Jr.; Stratmann, R. E.; Burant, J. C.; Dapprich, S.; Millam, J. M.; Daniels, A. D.; A. D. Kudin, A. D.; Strain, M. C.; Farkas, O.; Tomasi, J.; Barone, V.; Cossi, M.; Cammi, R.; Mennucci, B.; Pomelli, C.; Adamo, C.; Clifford, S.; Ochterski, J.; Petersson, G. A.; Ayala, P. Y.; Cui, Q.; Morokuma, K.; Malick, D. K.; Rabuck, A. D.; Raghavachari, K.; Foresman, J. B.; Cioslowski, J.; Ortiz, J. V.; Baboul, A. G.; Stefanov, B. B.; Liu, G.; Liashenko, A.; Piskorz, P.; Komaromi, I.; Gomperts, R.; Martin, R. L.; Fox, D. J.; Keith, T.; Al-Laham, M. A.; Peng, C. Y.; Nanayakkara, A.; Gonzalez, C.; Challacombe, M.; Gill, P. M. W.; Johnson, B.; Chen, W.; Wong, M. W.; Andres, J. L.; Gonzalez, C.; Head-Gordon, M.; Replogle, E. S.; Pople, J. A. *Gaussian 98*, revision A.7; Gaussian, Inc.: Pittsburgh, PA, 1998.

(43) Miertus, S.; Scrocco, E.; Tomasi, J. Electrostatic interaction of a solute with a continuum. A direct utilization of ab initio molecular potentials for the prevision of solvent effects. *Chem. Phys.* **1981**, *55*, 117.

(44) Hehre, W. J.; Radom, L.; Schleyer, P. v. R.; Pople, J. A. *Ab initio Molecular Orbital Theory*; Wiley: New York, 1986.

(45) Reed, A. E.; Curtis, L. A.; Weinhold, F. Intermolecular interactions from a natural bond orbital, donor−acceptor viewpoint. *Chem. Rev.* **1988**, *88*, 899−926.

(46) McPhail, D. B.; Hartley, R. C.; Gardner, P. T.; Duthie, G. G. Kinetic and stoichiometric assessment of the antioxidant activity of flavonoids by electron spin resonance spectroscopy. *J. Agric. Food Chem.* **2003**, *51*, 1684−1690.

(47) Bodini, M. E.; Copia, G.; Tapia, R.; Leighton, F.; Herrera, L. Iron complexes of quercetin in aprotic medium. Redox chemistry and interaction with superoxide anion radical. *Polyhedron* **1999**, *18*, 2233−2239.

(48) Makris, D. P.; Rossiter, J. T. Hydroxyl free radical-mediated oxidative degradation of quercetin and morin: a preliminary investigation. *J. Food Compos. Anal.* **2002**, *15*, 103−113.

(49) Awad, H. M.; Boersma, M. G.; Boeren, S.; van Bladeren, P. J.; Vervoort, J.; Rietjens, I. M. C. M. Quenching of quercetin quinone/quinone methides by different thiolate scavengers: stability and reversibility of conjugate formation. *Chem. Res. Toxicol.* **2003**, *16*, 822−831.

(50) de Souza, R. F. V.; De Giovani, W. F. Antioxidant properties of complexes of flavonoids with metal ions. *Redox Report* **2004**, *9*, 97−104.

(51) Moridani, M. Y.; Pourahmad, J.; Bui, H.; Siraki, A.; O'Brien, P. J. Dietary flavonoid iron complexes as cytoprotective superoxide radical scavengers. *Free Radical Biol. Med.* **2003**, *34*, 243−253.

Received for review July 4, 2006. Revised manuscript received November 15, 2006. Accepted November 30, 2006.

JF061864S